ARTICLE IN PRESS

Catalysis Today xxx (xxxx) xxx-xxx

FISEVIER

Contents lists available at ScienceDirect

Catalysis Today

journal homepage: www.elsevier.com/locate/cattod



Photoelectrochemical hydrogen production using CdS nanoparticles photodeposited onto Li-ion-inserted titania nanotube arrays

Unseock Kang^{a,b}, Kyu Jun Park^{a,b}, Dong Suk Han^c, Young-Min Kim^d, Seungdo Kim^d, Hyunwoong Park^{a,b,*}

- ^a School of Energy Engineering, Kyungpook National University, Daegu 41566, Republic of Korea
- b School of Architectural, Civil, Environmental, and Energy Engineering, Kyungpook National University, Daegu 41566, Republic of Korea
- Chemical Engineering Program. Texas A & M University at Oatar, Education City, P.O. Box 23874, Doha, Oatar
- ^d Department of Environmental Sciences and Biotechnology, Hallym University, Chuncheon 24252, Republic of Korea

ARTICLE INFO

Keywords: Solar fuel Artificial photosynthesis Heterojunction CdS ${ m TiO_2}$ nanotubes

ABSTRACT

This study reports the synthesis of cadmium sulfide (CdS) nanoparticles on Li $^+$ -inserted TiO $_2$ nanotube array (Li-TNA) to fabricate Li-TNA/CdS heterojunction electrodes for photoelectrochemical (PEC) hydrogen production under air mass (AM) 1.5 light and solar visible light ($\lambda > 420$ nm). For fabrication of the heterojunction, Li $^+$ is rapidly inserted into TNA pre-grown on Ti foil, and CdS is then photodeposited onto the Li-TNA electrodes for varying deposition times. Surface analyses reveal that sub-100-nm polycrystalline CdS particles partly cover the Li-TNA (length: ~ 800 nm, pore diameter: ~ 100 nm), enabling the heterojunction to utilize AM 1.5 light as well as visible light. In aqueous solutions of sulfide and sulfite, the Li-TNA/CdS exhibits an incident photon-to-current efficiency (IPCE) of $\sim 20\%$ ($\lambda = 420$ nm) while generating H $_2$ at a Faradaic efficiency of $\sim 100\%$. This PEC performance is superior to that of TNA/CdS, which is attributed to the Li $^+$ -enhanced charge transfer at the TNA/CdS interface. Electrochemical impedance analysis shows that the charge-transfer resistance of the TNA is reduced by $\sim 60\%$ by Li $^+$ insertion. Time-resolved photoluminescence decay profiles further reveal that the charge transfer in Li-TNA is completed within 0.8 ns, which is $\sim 33\%$ faster than that in TNA. The sample surface is analyzed using scanning electron microscopy, X-ray diffraction, energy-dispersive X-ray spectroscopy, X-ray photoelectron spectroscopy, and ultraviolet–visible spectroscopy, and the PEC behavior of the samples is discussed in detail.

1. Introduction

 ${
m TiO_2}$ nanotube array (TNA) is a promising material with unique one-dimensional porous nanoarchitecture that can be readily synthesized via electrical anodization of Ti foils in fluoride solutions at acidic pH [1–3]. The tube lengths and pore diameters are tunable by changing the processing parameters (applied voltages/currents and electrolyte) [2]. Upon bandgap (${
m E_g}$) irradiation, the photogenerated charge carriers are effectively separated along the tubular framework, enhancing the solar light harnessing efficiency [4–9]. Because of this unique physicochemical feature, TNA has been widely employed as a platform in energy-conversion processes using solar cells [10,11] and photocatalysis [12–15].

Coupling of CdS and TNA (TNA/CdS) is a representative application of TNA for solar visible light ($\lambda > 420$ nm) conversion [16–20]. The CdS and TNA binary heterojunction has several advantages, including the absorption of broadband sunlight because of the E_g of CdS

(\sim 2.4 eV) and cascaded charge transfer following the band levels of both semiconductors [21–25]. Nevertheless, challenges remain in terms of engineered interfacial design, accelerated charge transfer through the titania tubular framework, and robust contact between the two semiconductors [21].

In this study, two strategies have been adopted to design a high-efficiency heterojunction photoelectrocatalyst. First, CdS particles were loaded onto TNA via a photodeposition process [26]. In contrast to conventional loading methods, the photodeposition of CdS is initiated with the photogenerated electron transfer of TiO_2 , leading to nucleation and growth of CdS at the activated TiO_2 surface (Reactions (1)–(4); Scheme 1a).

$$TNA + h\nu \rightarrow e^- + h^+ \tag{1}$$

$$h^+ + D \rightarrow D^+ \tag{2}$$

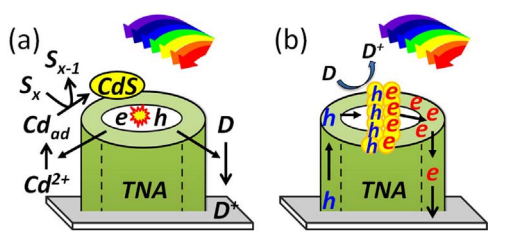
$$2e^- + Cd_{ad}^{2+} \rightarrow Cd_{ad} \text{ (in TNA)}$$
 (3)

http://dx.doi.org/10.1016/j.cattod.2017.08.049

Received 10 May 2017; Received in revised form 31 July 2017; Accepted 22 August 2017 0920-5861/ © 2017 Elsevier B.V. All rights reserved.

^{*} Corresponding author at: School of Energy Engineering, Kyungpook, National University, Daegu 41566, Republic of Korea. E-mail address: hwp@knu.ac.kr (H. Park).

U. Kang et al. Catalysis Today xxxx (xxxxx) xxxx—xxx



Scheme 1. Schematics of (a) CdS photodeposition mechanism on TNA and (b) photoinduced charge transfer on TNA/CdS heterojunctions. D refers to electron donor.

$$Cd_{ad} + S \rightarrow CdS \text{ (in TNA)}$$
 (4)

Whereas the employed photodeposition method is facile, tailoring the morphology of deposited CdS is rather difficult because the deposition proceeds via the reaction with the photogenerated charge carriers. Considering the diverse surface-specific redox activities of ${\rm TiO_2}$ [27], the specific surface regions where photoelectrons are generated and CdS grows should provide the most efficient electron transfer channel. Accordingly, the tubular configuration of the TNA (length and diameter) and the photodeposition time of CdS are important parameters in designing a high-efficiency heterojunction. Second, the TNA should exhibit high photoelectrochemical (PEC) performance under the bangap irradiation while providing an effective electron flow pathway. Thus, Li ions (Li $^+$) were intentionally inserted into the TNA (hereafter, Li-TNA) by applying negative potentials to the TNA electrodes in a Li $^+$ -rich solution (Reaction (5)):

$$TNA + xe^{-} + xLi^{+} \rightarrow Li-TNA$$
 (5)

Li $^+$ with an ionic diameter (\sim 0.068 nm) similar to H $^+$ can be inherently inserted into a TiO $_2$ lattice channel ($>\sim$ 0.07 nm) [28] at a level of \sim 10¹⁸ Li $^+$ cm $^{-2}$ -TNA [15]. Li $^+$ insertion results in decreases in the photoluminescence and charge-transfer resistance, whereas the incident photon-to-current efficiency (IPCE) and hydroxyl (OH) radical generation efficiency of TNA are enhanced by \sim 2.5 fold [15]. This effect can be attributed to the charge compensation of photogenerated Ti $^{3+}$ by surrounding Li $^+$, while Li $^+$ -Ti $^{3+}$ species inhibit the recombination of charge carriers [29].

With this in mind, we aimed to synthesize Li-TNA/CdS heterojunction electrodes and optimize their performance under simulated irradiation (AM 1.5 and visible light (> 420 nm) of AM 1.5). Surface characterizations, including scanning electron microscopy (SEM), X-ray photoelectron spectroscopy (XPS), X-ray diffraction (XRD), and ultraviolet–visible (UV–vis) spectroscopy, were performed, and the PEC performance of the heterojunctions was systematically investigated in terms of IPCE and $\rm H_2$ evolution in sulfide and sulfide/sulfite solutions. Finally, the time-resolved photoluminescence emission of the samples was analyzed to gain insight into the charge-transfer kinetics.

2. Experimental

2.1. Preparation of materials

TNA was prepared following a modified anodization method reported elsewhere [14,15,30]. In brief, a Ti sheet (0.127-mm thick, 99.7% pure, Aldrich) was cut into small pieces (1.5 cm \times 3.0 cm), which were ultrasonically cleaned in ethanol for 10 min in an ultrasonic bath (WiseClean, 40 kHz, 100 W) and rinsed with deionized water. Then, a couple of a Ti piece and a stainless steel plate (distance \sim 3 mm) was immersed in an aqueous solution of NaF (0.28 M) and H₃PO₄ (1.0 M), and a direct current (DC) voltage of +20 V was applied to the Ti piece with respect to the stainless steel for varying times (1–6 h) with stirring of the solution with a magnetic bar. Unless otherwise specified, the anodization time was fixed at 4 h (denoted TNA-4). After washing with high-purity acetonitrile, the as-obtained

samples were annealed at 500 °C for 6 h in the presence of atmospheric air to obtain crystalline TNA. For comparison, the Ti substrate was annealed without the anodization treatment (denoted TNA-0). The assynthesized TNA samples were immersed in 1 M LiClO $_4$ (Aldrich), and a potential of $-1.4\,\mathrm{V}$ versus a saturated calomel electrode (SCE, reference electrode) was applied to the substrate for 3 s using a potentiostat/galvanostat (Versastat 3-400, Princeton Applied Research) to insert Li $^+$. Pt foil was used as the counter electrode.

For the deposition of CdS particles, TNA and Li-TNA samples were immersed in ethanol containing S_8 (0.172 mM, Aldrich) and Cd(ClO_4)_2 (1.38 mM, Aldrich) over 1 h [26]. Then, the samples were irradiated with UV light (1.4-W black light generating wavelengths of 315–400 nm, OPECS) for varying times (0–3 h). Unless otherwise specified, the photodeposition time was 1.5 h (denoted CdS-1.5). Finally, the CdS-deposited TNA and Li-TNA were annealed at 450 $^{\circ}\text{C}$ for 30 min in the presence of air. The amount of CdS loaded was estimated to be similar between TNA and Li-TNA (\sim 10% difference).

2.2. Photoelectrochemical tests

The photoelectrochemical (PEC) behavior of the samples was examined with a typical three-electrode configuration (SCE: reference electrode, Pt gauze: counter electrode) using the potentiostat/galvanostat. All three electrodes were immersed in an air-tight single glass cell containing aqueous solutions of sulfide (1 M, Na₂S, Aldrich) alone or a sulfide and sulfite (Na₂SO₃, Aldrich) mixture (each 0.5 M). A certain fraction of the sample surface (0.25 cm²) was exposed to the electrolyte and irradiated. A 150-W Xe arc lamp (ABET Technologies, U.S.A.) equipped with an air mass 1.5 (AM 1.5G) filter was used as the light source. For visible light, a long-wave band pass filter $(\lambda > 420 \text{ nm}, \text{Newport}, \text{U.S.A.})$ was inserted between the light source and electrochemical cell. Potentials ranging from -0.5 to +1.5 V vs. SCE were swept at a scan rate of 20 mV s⁻¹ in the dark or under irradiation. If necessary, constant potentials (-0.5, 0, and +0.5 V vs. SCE) were applied. For the impedance analysis (Nyquist plots), alternating current (AC) impedance measurements were performed through application of a bias potential of 0 V vs. SCE in sulfide or sulfide/sulfite solutions with a frequency range of 1 MHz to 0.01 kHz and an AC voltage of 10 mV rms (Ivium Tech., U.S.A.).

The incident photon-to-current efficiency (IPCE) was determined in aqueous sulfide and sulfide/sulfite solutions with the same three-electrode system using a 300-W Xe lamp (Newport). Monochromatic light was produced by a CS 130 monochromator with a 10-nm bandpass, and the output power was measured using a Si photodiode detector (Newport). The IPCE was then calculated as follows:

IPCE (%) =
$$(1239.8/\text{V nm} \times I_{\text{ph}}/\text{mA cm}^{-2}) \times 100/(P_{\text{mono}}/\text{mW cm}^{-2} \times \lambda/\text{nm}),$$

where $I_{\rm ph}$, $P_{\rm mono}$, and λ refer to the photocurrent density at 0 V vs. SCE, monochromated illumination power intensity, and wavelength, respectively.

For hydrogen evolution tests, N_2 (99.9%) was purged through the solutions for 1 h, and the sample electrodes were held at a constant potential of -0.5 V vs. SCE. After irradiation, the headspace H_2 evolved from water was quantified using a gas chromatography system equipped with a thermal conductivity detector (GC-TCD, Agilent 7820, U.S.A.) with a 5-Å molecular sieve column. A standard H_2 gas was allowed to flow through the GC-TCD, and a standard linear fit between the H_2 gas concentration and corresponding spectral area was obtained.

2.3. Surface characterization and time-resolved photoluminescence analysis

XRD (Rigaku D/Max-2500) and XPS (VG Scientific, ESCA LAB 220i XL, MgK α source) were employed to examine the crystalline patterns and binding states of the sample elements, respectively. Field-emission

Download English Version:

https://daneshyari.com/en/article/6504718

Download Persian Version:

https://daneshyari.com/article/6504718

<u>Daneshyari.com</u>